Fusion of images obtained from EIT and MRI

J.L. Davidson, R.A. Little, P. Wright, J. Naish, R. Kikinis, G.J.M. Parker and H. McCann

A novel and effective methodology of combining images obtained by both electrical impedance tomography (EIT) and magnetic resonance imaging (MRI) data is described. Co-registered and fused image results for an example laboratory phantom based on the polysaccharide gel TX151 are presented. Bespoke software was used to convert an EIT dataset into a form consistent with *3D-Slicer*, a powerful software package used for visualisation and image analysis. The data fusion provides a highly effective method of directly comparing EIT images, which typically have good temporal resolution and relatively poor spatial resolution, with those obtained with MRI, which has relatively poor temporal resolution but excellent spatial resolution.

Introduction: Clinicians are frequently faced with patient care challenges that require knowledge of both detailed anatomical information and the performance of an organ's key functionality. Examples include critical treatment of brain trauma, cardiac disease, tumours in many locations (e.g. brain, liver, kidney, lungs) and pulmonary conditions. Imaging modalities capable of rapid scanning (e.g. electrical impedance tomography (EIT)) typically lack the spatial resolution of MRI or X-ray CT, which is often crucial in understanding organ functionality and/or the progression of a disease. The inescapable conclusion is that with present technologies, the optimum combination of anatomical and functional imaging requires characterisation with more than one imaging modality. Initially, our target application is functional EIT of the lung but the data fusion process could be exploited in other areas such as multi-modal neurophysiology, and also in engineering process research such as the study of catalytic fluidised-bed dynamics. In the present application, this combination of imaging modalities enables an accurate and quantitative comparison of the structural and functional information provided by EIT with the complementary structural and functional information provided by MRI. Analysis of an example dataset demonstrates the fusion of EIT and MRI data from an inanimate gel-based phantom using *Confeitir* (CONverter of Functional Electrical Impedance Tomography Images for Registration) software [1] and *3D-Slicer* software [2].

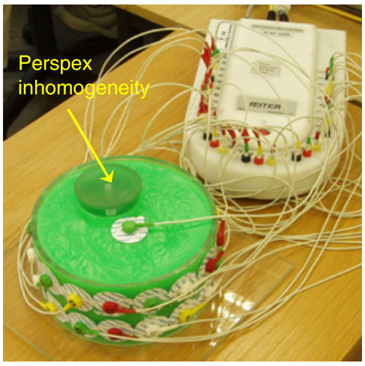

Fig. 1 *TX151 gel phantom with Perspex inhomogeneity of 11° taper during EIT capture*

A tissue-realistic phantom and data acquisition: A phantom of diameter 170 mm and height 85 mm was constructed using TX151 polysaccharide gel (Oil Center Research, La Fayette, LA). This is a tissue-realistic material which has previously been used in the context both of EIT and of MRI [3]. To every 1 litre of deionised water, 120 g TX151 was added and the result was thoroughly mixed in a blender before being poured into a cylindrical Perspex mould and allowed to set. Apertures at 25 and 65 mm height on the cylinder wall were located in the mould so that Ag/AgCl EEG electrodes could be affixed to the phantom for EIT measurements. The electrodes were arranged in two rings of 16 with an additional reference electrode placed top-centre of the phantom. EIT data were captured using the EIT sub-system of fEITER (*functional Electrical Impedance Tomography of Evoked Responses*) [4], a biomedical EIT instrument developed for use in the operating room which complies with medical standard BS EN 60601-1:2006. The instrument operated at 100 frames per second (fps) and used an opposite-electrode strategy involving eight current projections per electrode ring. EIT measurements were acquired for (i) a reference condition which included an MRI-transparent tapered inhomogeneity and (ii) the same phantom after the replacement of the inhomogeneity with an exact metal copy. This method provided 420 horizontal difference-voltage measurements per frame between adjacent (non-current injecting) electrode pairs for EIT image reconstruction, without changing the volume integrity of the TX151 gel. The arrangement is shown in Fig. 1. In such a laboratory benchtop situation, the noise on the rms voltage difference measurements is typically 3 or 4 μV [4].

For MRI acquisitions, a 3D T_1-weighted FFE/SPGR (fast field echo/spoiled gradient echo) acquisition [5] was conducted on a 1.5 T Philips Achieva scanner (Philips Healthcare, Best, The Netherlands). This provided a high-fidelity spatial representation of the phantom structure. The reconstructed MRI image matrix had $144 \times 144 \times 57$ volume elements (voxels) of dimensions $1.74 \times 1.74 \times 2.06$ mm. Additionally, the phantom was modelled using *NetGen* [6] to give a tetrahedral mesh of 12966 elements for EIT image reconstruction which used a difference-imaging technique based on linear conjugate gradients and *EIDORS 3D* [7].

Conversion of EIT solution to voxel space: The Manchester *Confeitir* [1] software package was used to convert the reconstructed EIT data from the resulting irregular tetrahedral mesh into a matrix with 2 mm-cubic isotropic voxels. The *Confeitir* algorithm iterates over a large number of (arbitrarily defined and irregular) tetrahedra and identifies voxels which have their centres within its boundary. This is more computationally challenging than finding the nearest-neighbour centroid for each voxel, but produces a more realistic result, as the simpler method may populate voxels with the solutions of neighbouring tetrahedra (e.g. where a short and fat simplex is located next to a long and thin simplex).

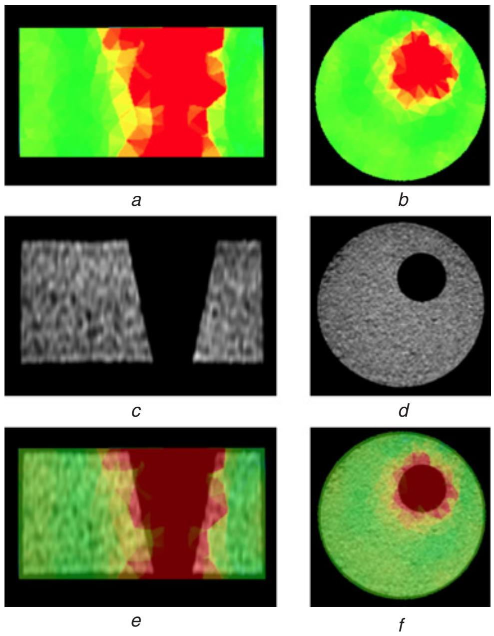

Fig. 2 *3D-Slicer images showing axial and coronal slices of EIT reconstruction of phantom compared to MRI ground truth*

a,b EIT reconstruction in false-colour
c,d MRI data
e,f Same slices with EIT reconstruction (semi-transparent in false-colour) overlaid on the greyscale MRI data

3D data fusion and visualisation: The fusion of images requires a sophisticated and robust software platform. In this study, the open-source software package *3D-Slicer* was used to manipulate and visualise the resulting data. The software provides a flexible platform from which to analyse and view medical image datasets and is ideally suited to tailoring for specific research questions. For the presented TX151 phantom example, only the built-in functions of *3D-Slicer* were required. The MRI-derived dataset was in the form of DICOM files, whilst the EIT-derived conductivity change measurements, after conversion to a cubic matrix, were represented as *Mayo Clinic Analyze 7.5* format files. Both the MRI and EIT data were imported into *3D-Slicer* and manual translation and rotation were applied until they were visually aligned. The built-in volume rendering module was used to create a model of the phantom from the MRI volume to aid visualisation of the 3D structure of the phantom. Fig. 2 shows some of the resulting axial and coronal images from the two datasets as visualised using *3D-Slicer*. Figs. 2*a* and *b* show the EIT dataset and clearly show the conical imhomogeneity. The remaining rows are of slices showing the MRI data alone (Figs. 2*c* and *d*) and a co-registered overlay of the EIT dataset on the MRI data (Figs. 2*e* and *f*). Fig. 3 illustrates a combined visualisation of the two datasets, with axial and coronal slices of the EIT data combined with a 3D volume rendering of the MRI dataset. A visual inspection of these images suggests good correspondence between the two modalities, clearly showing the top-to-bottom tapering that was physically present in the original phantom. For the presented phantom and reconstruction method, visual inspection of the two datasets suggests a spatial resolution of about 10 mm^3 in the EIT images.

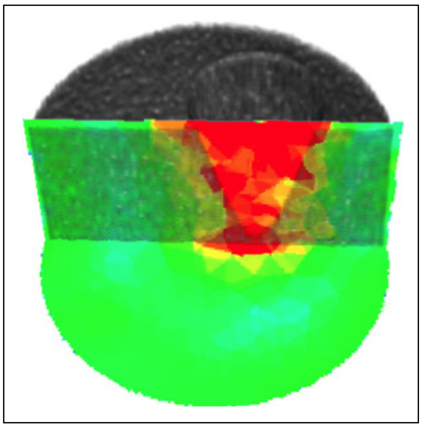

Fig. 3 *3D-Slicer image of fused EIT and MRI data acquisition of TX151 phantom showing axial and coronal slices of EIT data (colour scale) cutting through inhomogeneity, overlaid on a volume rendering of MRI dataset (greyscale)*

Conclusion and future work: The concept of EIT and MRI data fusion using *Confeitir* and *3D-Slicer* has been successfully demonstrated. Further analysis and phantom tests will enable a more systematic quantitative determination of EIT spatial fidelity. The fusion of EIT and MRI data is an essential step in the development of combined dynamic lung function imaging with human EIT and MRI data.

Acknowledgments: This work is funded via the RCUK Science Bridges award, EPSRC Ref: EP/G041733/1. All MRI scanning was performed in the Manchester Wellcome Trust Clinical Research Facility.

31 January 2012
doi: 10.1049/el.2012.0327
One or more of the Figures in this Letter are available in colour online.

J.L. Davidson, P. Wright and H. McCann (*School of Electrical and Electronic Engineering, University of Manchester, United Kingdom*)

E-mail: j.davidson-2@manchester.ac.uk

R.A. Little, J. Naish and G.J.M. Parker (*Imaging Sciences, Biomedical Imaging Institute, Manchester Academic Health Sciences Centre, University of Manchester, United Kingdom*)

R. Kikinis (*Surgical Planning Laboratory, Brigham and Women's Hospital, Harvard Medical School, Boston, MA, USA*)

References

1 McCormick, D., Davidson, J.L., and McCann, H.: 'Conversion of EIT brain images for co-registration'. Proc. 13th Int. Conf. on Electrical Bioimpedance and the 8th Conf. on Electrical Impedance Tomography, Graz, Austria, 2007, pp. 384–387, ISBN 978-3-540-36839-7
2 Pieper, S., Halle, M., and Kikinis, R.: '3D SLICER'. Proc. 1st IEEE Int. Symp. on Biomedical Imaging: From Nano to Macro, 2004, Vol. 1, pp. 632–635, (see http://www.slicer.org)
3 Mazzara, G.P., Briggs, R.W., Wu, Z., and Steinbach, B.G.: 'Use of a modified polysaccharide gel in developing a realistic breast phantom for MRI', *Magn. Reson. Imaging*, 1996, **14**, pp. 639–648
4 McCann, H., Ahsan, S.T., Davidson, J.L., Robinson, R.L., Wright, P., and Pomfrett, C.J.D.: 'A portable instrument for high-speed brain function imaging: fEITER'. Proc. 33rd Annual Int. Conf. of the IEEE Engineering in Medicine and Biology Society, (EMBS), Boston, MA, USA, 2011, pp. 7029–7032
5 Bernstein, M.A., King, K.F., and Zhou, X.J.: 'Handbook of MRI pulse sequences' (Elsevier Academic Press, 2004, 1st edn)
6 Schöberl, J.: 'NETGEN – an advancing front 2D/3D-mesh generator based on abstract rules', *Comput. Vis. Sci.*, 1997, **1**, pp. 41–52, (http://www.hpfem.jku.at)
7 Polydorides, N., and Lionheart, W.R.B.: 'A Matlab based toolkit for three-dimensional electrical impedance tomography: a contribution to the EIDORS project', *Meas. Sci. Technol.*, 2002, **13**, pp. 1871–1883